JJEES

Jordan Journal of Earth and Environmental Sciences

Volume 6, Number 2, December, 2014
ISSN 1995-6681
Pages 45- 51

Removal of Aqueous Chromium (III) Ions Using Jordanian Natural Zeolite Tuff in Batch and Fixed Bed Modes

Ahmad M. Al-Haj-Ali* and Lana M. Marashdeh

Dept. of Chemical Engineering, University of Jordan

Received 3 September, 2014; Accepted 25 December, 2014

Abstract

The present study was undertaken to evaluate the capability of natural zeolite tuffto remove Cr(III) ions from aqueous solutions by physical chemical method under specified conditions. Investigationsinvolved shake-flasks experiments conductedusing 1.0-8.0 g/L doseof 355-500 µm zeolite particles in solution of 50 mg Cr(III)/L at initial pH of 4.0 and 22°Cas well as fixed-bedexperiments conducted using 4.8-14.4 cm bed height, 5.66-12.45 solution velocity, 50-100 mg/L initial metal concentration, size cuts in the range +355-850µmand initial pH of 4.0-5.5. The equilibrium adsorption capacity reached 19.6 mg/g and the data fitted well both Langmuir and Redlich-Peterson isotherms. Break points up to 2.5 hours were obtained at 5% breakpoint using fixed-beds of zeolite at the lower metal concentration and solution velocity but higher pH and bed depth. Mechanism of removal appears to be ion exchange of $Cr(OH)^{2+}$at pH≤ 6.0 and adsorption on zeolite surface of fine $Cr(OH)_3$ precipitate at pH> 6.0.

Keywords: Trivalent chromium, natural zeolite, adsorption isotherms, breakthrough curves, Jordan.

1. Introduction

Being used in many very important industrial applications, Chromiumplays a key role in many industries such as leather tanning, metal electroplating and other surface finishing, pigments, paints, textile, wood preservation, fire-retardant formulas, reaction catalysis, batteries, magnetic tapes and corrosion inhibition (Kirk-Othmer Encyclopedia, 2007). From these industries, there is a substantial disposal of chromium-containing process effluents and sludges that contaminate the soil, surface water and underground water before eventually entering the human food chain (Adriano, 2001).Chromium may exist in several oxidation states of which 0, 3 and 6 are stable enough to occur in the environment. Cr(VI) is much more soluble and due to the mobility of its species in water it constitutes a high health and environmental hazard. Cr(III) is the most chemically stable and best known oxidation state of chromium. In the presence of manganese oxides, Cr(III) can be easily oxidized to Cr(VI). According to Stumm and Morgan (1996), the interaction of trivalent chromium with the environment involves various chemical and physical processes including hydrolysis, complexation, redox reactions and adsorption.

The discharge limits from industrial effluents vary according to the fate or application of wastewater. For example, the maximum allowable concentration of total chromium in the Jordanian wastewater (both industrial and treated domestic sewage) standards is 0.01 mg/L for reuse in irrigation and discharge to streams and lakes; 0.02 mg/L for underground water recharge and 0.07 mg/L for discharge to the sea. Drinking water guideline value for Cr(III) recommended by World Health Organization (WHO) is 0.005 mg/L (WHO, 2011), which is adopted by the Jordanian standard for drinking water. Two engineering techniques for heavy metal removal are usually applied, namely chemical precipitation and ion exchange. These methods suffer from disadvantages such as non-selectivity, high cost and waste disposal problems. Natural zeolites are crystalline microporousaluminosilicates with well-defined structures that consist of a framework formed by tetrahedra of SiO_4 and AlO_4 connected through oxygen atoms. The frame-work contains channels and cavities with molecular dimensions from 0.3 to 1 nm occupied by alkaline and alkaline earth metal cations as well as water molecules. These cations possess the ability to move freely and can be exchanged by more selective cations from aqueous solutions (Wang and Peng, 2010).

Fixed beds of zeolite may be used as packing materials in subsurface barriers to control ground water pollution (Obiri-Nyarkoa *et al*., 2014). These applications are stimulated by the non-toxic nature of zeolites as well as their availability in many countries at low cost. Application of natural zeolites for the removal of heavy metals such as Pb(II), Cd(II), Ni(II), Zn(II), etc. has been reported in several studies considering both batch equilibrium and dynamic fixed-bed column experiments (Alvarez-Ayuso *et al*., 2003; Al-Haj-Ali and Al-Hunaidi, 2004; Baker *et al*., 2009; Karatas, 2012; Malamisa and Katsou, 2013).

In northeastern and central parts of Jordan, large deposits of natural zeolites, produced by alteration of basaltic glass, are present and estimated as geological reserves at 170 million tons. Currently, these minerals (mostly phillipsite and chabazite) are being mined and made commercially available for agricultural applications where they are used as a soil conditioner (Natural Resources Authority, 2006). Environmental applications of Jordanian zeolites, as

---

* Corresponding author. e-mail: ahmad.ay55@gmail.com

adsorbents and ion exchangers for pollutant removal, have been the subject of investigation over the last two decades. Published studies over the past two decades have shown that Jordanian zeolite tuffs, from different locations in Jordan, are efficient adsorbents for heavy metal removal from aqueous solutions and industrial wastewater (Al-HajAli and El-Bishtawi, 1997; Ibrahim *et al*., 2002; Taamneh and Al Dwairi, 2013).

The main objective of this study is to evaluate the ability of a major type of natural Jordanian zeolite, namely, Phillipsite tuff for the removal of Cr(III) ions under various adsorption conditions of zeolite and solution, both in batch and fixed-bed column modes. In particular, the adsorption capacity, mechanism and breakthrough times are sought for further consideration of the mineral application.

2. Methodology

2.1. Materials

The zeolite tuff used in this work was mined from Jabal Aritayn area in the northeastern part of Jordan and supplied by the Natural Resources Authority of Jordan. X-Ray Diffraction (XRD) analysis has shown that the raw zeolite tuff is rich in phillipsite and calcite ($CaCO_3$) is the major non-zeolitic impurity (Fig. 1).

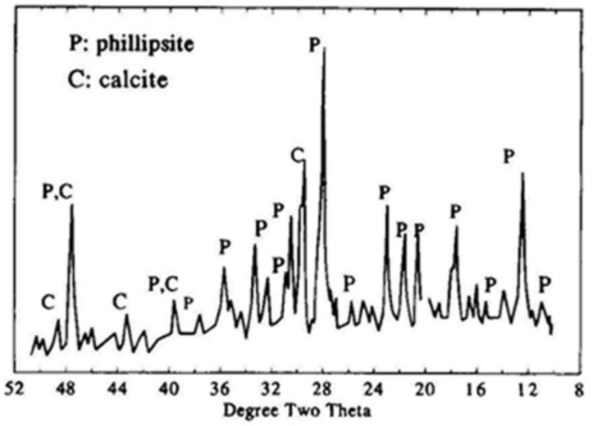

Figure 1: X-ray diffraction chart of zeolite tuff (P: phillipsite, C: calcite)

A scanning electron microscope of the mineral is shown in Fig. 2, indicating the heterogeneous surface and irregular shape of the mineral particles.

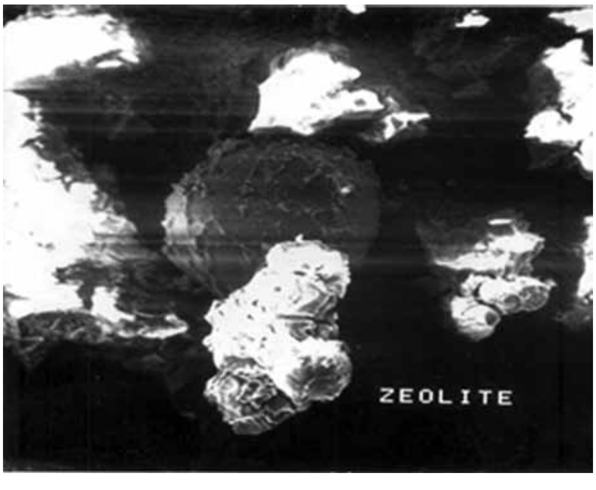

Figure 2: Scanning electron micrograph (SEM) of powdered zeolite

The mineral was crushed using a Jaw crusher and sieved into different size cuts; those of 355-500, 500-710 and 710-850 μm were selected for metal uptake experiments. These size cuts were washed with distilled water to remove all fines, immersed in 25g/L analytical grade sodium chloride solution for 48 hours to convert the zeolite into Na-form. The NaCl solution was then decanted and zeolite sample washed gently with distilled water to remove trace salt. Finally, the zeolite sample was oven-dried overnight at 100°C.

Table 1: Physical Properties of Unsieved and Size Cuts of Zeolite

Unsieved Zeolite: True Density: 2.380 g/cm³ Bulk Density: 1.035 g/cm³ Color: Yellowish Brown				
Size Range	Langmuir Surface Area (m^2/g)	BET Surface Area (m^2/g)	Total Pore Volume (cm^3/g)	Avg. Pore Diameter (Å)
355-500 μm	124	92.0	4.02×10^{-2}	1.75
710-850 μm	120	90.0	3.90×10^{-2}	1.75

Various physical properties of unsieved zeolite and some size cuts are given in Table 1. Langmuir and Brunauer Emmett Teller (BET) surface areas and total pore volume and average pore diameter were determined for zeolite sieve cuts using a Quanta chrome Autosorb automated gas sorption system. Data are calculated and reported using Autosorb 1 program for nitrogen at 77K. Also, the chemical composition of raw zeolite (as received) was obtained by x-ray fluorescence (XRF) analysis and is given in Table 2.

Table 2: Chemical Composition of Raw Unsieved Zeolite (Weight Percent)

SiO_2	Al_2O_3	FeO	CaO	MgO	K_2O	Na_2O	TiO_2	Other
34.2	10.57	7.02	11.35	7.28	2.00	1.65	1.23	0.33

Analytical grade chromium chloride was used as source for Cr(III) ions. Stock solutions of 1000 mg Cr(III)/L were prepared by dissolving the exact weight of $CrCl_3.6H_2O$ in distilled-deionized water and used to provide the desired Cr(III) ion concentration by proper dilution. Glassware was cleaned by detergent and double rinsed thoroughly by tap water and distilled-deionized water.

2.2. Procedure and Analysis

2.2.1 Equilibrium Experiments

Adsorption capacity was determined by shake-flask batch experiments. A volume 150 mL of solution containing 50 mg/L was placed in a 250 mL Erlenmeyer flask. The initial pH was adjusted to a specified initial value of 4.0 while the final pH was left uncontrolled to determine how it changes during the process. An accurately-weighed zeolite mass in the range 0.12-1.2 g was added to the solution, thus making slurry concentration in the range 1.0- 8.0 g/L.A series of such flasks was then agitated at a constant speed in a laboratory shaker at room temperature of 22°C until equilibrium is attained, followed by separation of zeolite particles by filtration. A sample of the solid-free solution was analyzed for Cr(III) remaining concentration using UNICAM atomic absorption spectroscopy. Meanwhile, the final pH of the solution was measured using a calibrated pH meter.

2.2.2 Column Experiments

The apparatus used consists of a bench-mounted glass column, 1.5cm inside diameter and 90cm height. The column is gently packed with different masses of zeolite which provide different bed depths. The feed solution is pumped from a glass storage tank to an overhead constant-level tank made of plexi-glass and fed to the column through a glass flow meter. Flow control is achieved by valves fitted at the top and at the bottom of column. Samples from effluent solution are withdrawn at predetermined time intervals and analyzed for metal ion concentrations using by atomic absorption spectroscopy. Experimental column variables and their tested ranges are given in Table 3.

Table 3: Breakpoint time in zeolite beds at various experimental conditions

Expt. #	Solution velocity, u (cm/min)	Bed Depth, H (cm)	Initial Cr(III) Concentration, Co (mg/L)	Particle Size Cut (µm)	5 % Breakpoint time, tB(min)
1	12.45	14.4	50	355-500	15
2	8.49	14.4	50	355-500	150
3	5.66	14.4	50	355-500	150
4	5.66	9.6	50	355-500	75
5	5.66	4.8	50	355-500	30
6	8.49	14.4	75	355-500	60
7	8.49	14.4	100	355-500	30
6	8.49	14.4	50	500-710	50
7	8.49	14.4	50	710-850	30

3. Results and Discussion

3.1. Adsorption Isotherms

The adsorptive capacity of a solid is concluded from equilibrium sets of data that need to be fitted to mathematical models to facilitate design of adsorption systems and broaden their application. Data on equilibrium uptake were fitted to the popular models of adsorption isotherms, namely; Langmuir, Freundlich and Redlich-Peterson equations which are favored by most researchers because of interpretable parameters and simple expression. These models have the following non-linear forms, respectively (Redlich and Peterson, 1959):

$$q_e = Q_L.b.C_e / (1 + b.C_e) \quad (1)$$

$$q_e = K_F. C_e^{1/n} \quad (2)$$

$$q_e = A_R.C_e / (1 + B_R.C_e)^g \quad (3)$$

The parameters of each isotherm model are obtained from the slope and intercept of the linearized form of the respective model. The Redlich-Peterson isotherm combines both Langmuir and Freundlich isotherms thus suggesting a hybrid mechanism of adsorption rather than the ideal monolayer adsorption. It has three constants, namely, A_R, B_R and g, which characterize the isotherm. In the above equation, constant "g" is the exponent, which lies between 0 and 1. Experimental data taken at an equilibrium time of 120 hours and the model predictions of q_e are compared in Figure 3, where Redlich-Peterson model showed the best fit. Fig. 4 confirms this by linear plot of C_e/q_e versus C_e^g with a correlation coefficient of 0.99.

The parameters of the three adsorption isotherms were obtained from linear regression analysis of equations 1, 2 and 3 and their values are given in Table 4 along with the correlation coefficients and standard deviations of error. These values were then inserted in the original isotherm models to predict the equilibrium uptake which yielded the following equations:

$$q_e = 19.6\, C_e / (1 + 0.13 C_e) \quad (4)$$

$$q_e = 5.41\, C_e^{3.65} \quad (5)$$

$$q_e = 6.31\, C_e / (1 + 0.93\, C_e)^{0.75} \quad (6)$$

Table 4: Results of regression analysis for data fitting to adsorption isotherms

Langmuir	Fruendlich	Redlich-Peterson
$Q_L = 19.6$ $b = 0.13$ $R^2 = 0.96$	$K_F = 5.41$ $n = 0.274$ $R^2 = 0.90$	$A_R = 6.31$ $B_R = 0.93$ $g = 0.75$ $R^2 = 0.99$

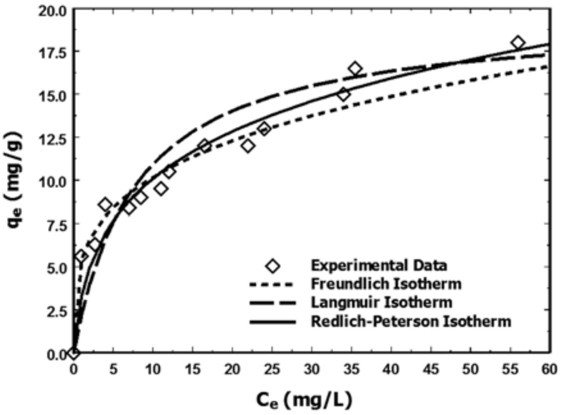

Figure 3: Equilibrium uptake modeled by different adsorption isotherms

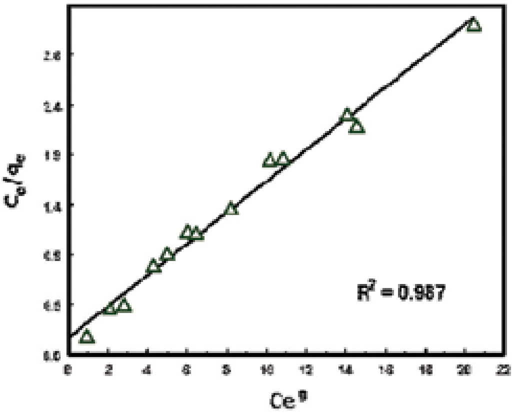

Figure 4: Linearized Redlich-Peterson model for Cr(III) adsorption by natural zeolite tuff

Figs. 3 and 4 clearly show that Redlich-Peterson model represents the experimental data quite well compared to the two other models. This is an indication that Cr(III) uptake mechanism is not purely monolayer coverage typically represented by Langmuir isotherm which is associated with chemisorption but rather a combination of both ion exchange and physical adsorption. Although the Redlich-Peterson model represented the experimental data better than Langmuir isotherm, the latter remains a tool to estimate the maximum adsorption capacity.

3.2. Final pH

In Fig. 5, the final pH attained in solution at equilibrium is plotted as a function of zeolite dose. The initial pH was adjusted at a fixed value of 4.0 and left to change with process

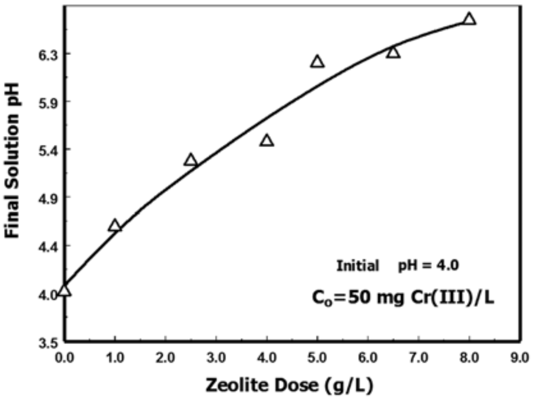

Figure 5: Equilibrium pH as a function of zeolite dose

variables. The increase of pH is mainly attributed to the release of alkaline metal ions from zeolite surface. In addition to naturally existing alkaline metals in zeolite, the major alkaline ion released during adsorption is sodium (Na^+) added in the zeolite pretreatment step. Uptake of cations, e.g. Cr^{3+} and H_3O^+ (hydronium) ions by zeolite would reduce solution acidity. Moreover, dissolution of alkaline impurities in zeolite tuff, mainly $CaCO_3$ (appeared as a significant constituent in the XRD analysis) is also responsible for part of the pH rising.

3.3. Breakthrough Curves

The effects of solution flow-rate, bed depth, initial concentration of Cr(III) ions in the feed, zeolite particle size and initial pH on the sorption behavior of Cr(III) ions are presented and discussed. The 5% break point time is taken as an indicator of zeolite bed efficiency and defined as the time required to reach the break point where C/C° = 0.05. It is well known, from the mass transfer theory of breakthrough curves (Reynolds and Richards, 1996), that the higher the breakpoint time, the higher is the adsorbate removal and the more efficient is the bed. Breakpoint time (t_B) values obtained from various breakthrough curves describing Cr(III) uptake by zeolite bed are given in Table 3 along with the respective column parameters.

3.3.1 Effect of Bed Depth

In Fig. 6, the bed depth was varied, keeping all other parameters constant as in given in Table 3. Obviously, the highest value of t_B (150 min) was obtained using the highest bed depth (14.4 cm). Decreasing the bed depth while keeping the solution velocity constant at 5.66 cm/min resulted in significantly shorter breakpoint times (75 minutes at 9.6 cm and only 30 minutes at 4.8cm). For the latter case, the C/C° versus time plot does not give the typical S-curve. It is concluded that at the conditions tested, a bed depth less than 9.6 cm (zeolite mass less than 20 g) will not give a satisfactory sorption performance.

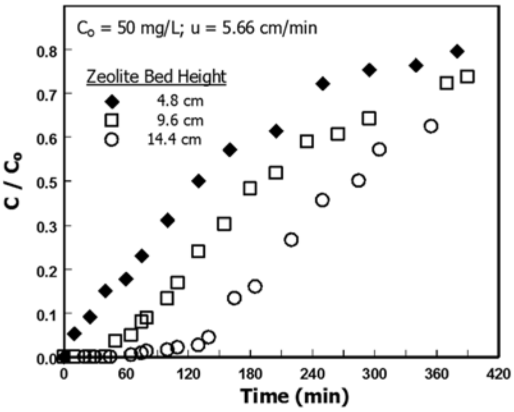

Figure 6: Breakthrough curves at variable bed depth

3.3.2 Effect of Solution velocity

Breakthrough curves, obtained using three solution velocities keeping other parameters constant (zeolite mass = 30 g equivalent to 14.4 cm of bed depth), are shown in Fig. 7. At 5% break point, t_B value of 150 minutes was obtained at flow rates of 5.66 and 8.49 cm/min, indicating a relatively efficient bed. However, the bed performance is unsatisfactory at higher solution velocities where the breakpoint time is very short (15 minutes) at 12.45cm/min. The effect of solution velocity on bed adsorption capacity is due to the difference in residence time of solution in contact with zeolite particles.

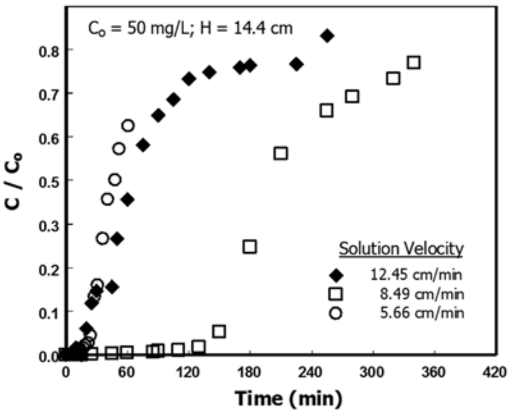

Figure 7: Breakthrough curves at variable solution velocity

3.3.3 Effect of Initial Cr(III) ion Concentration

Fig. 8 shows the effect of Cr(III) ion concentration in feed solution, C°, on breakpoint time is shown in maintaining a constant flow rate at 8.49 cm/min and bed depth at 14.4 cm. The slopes of breakthrough curves decreased as C° decreased, indicating better sorption behavior at the lowest C° of 50 mg/L, where the 5% breakpoint time reached 150 minutes compared to 60 and 30 minutes at the higher C° values of 75 and 100 mg/L, respectively.

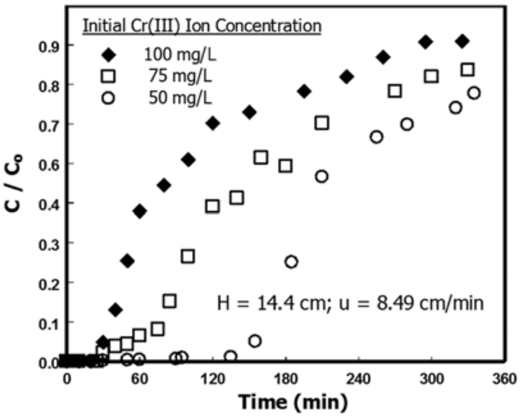

Figure 8: Breakthrough curves at variable initial Cr(III) concentration

3.3.4 Effect of Zeolite Particle Size

Fig. 9 shows that as the particle size of the zeolite bed increased, the 5% breakpoint time decreased. Values of t_B of 150, 50 and 30 minutes were obtained by when 355-500, 500-710 and 710-850 μm sieve cuts were used. Therefore, lower zeolite size fractions are preferred since they produce

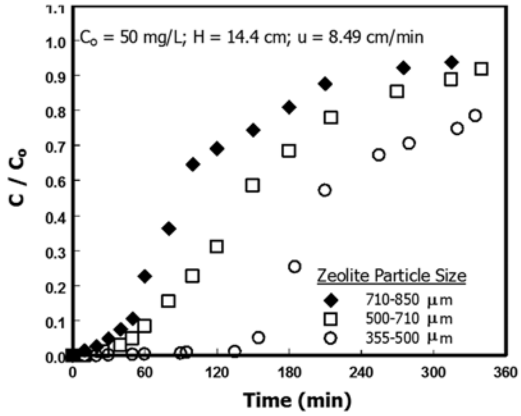

Figure 9: Breakthrough curves at variable zeolite particle size

higher surface area available for adsorption. In addition, the ion exchange capacity may change with particle size due to the variation of zeolite grade in the tuff mineral (Al-Haj Ali and El-Bishtawi, 1997; Ibrahim and Jbara, 2009). In practical applications, very small particles should not be used as they may cause pressure drop across the bed to rise, slow the process and increase energy consumption. If t_B is assumed to be a valid criteria for comparison, it can be concluded that particle size must be carefully selected to optimize Cr(III) removal capacity of zeolite beds with their operability.

3.3.5 Changes in pH

The changes of pH during chromium ion uptake in a typical breakthrough experiment are shown in Fig. 10. Starting with feed solutions initially adjusted to pH 4.0, the pH during sorption has risen sharply in the first 10 minutes to 6.9 then declined slowly and leveled off at 5.6. It is clear that the final pH is always higher than that of the particle-free solution.

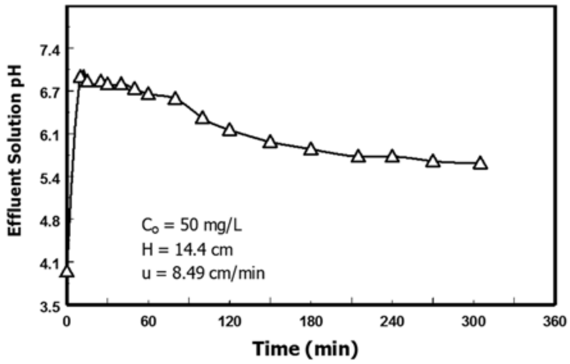

Figure 10: Change in effluent pH with time in fixed-bed

To explain this observation, several processes that occur during metal-zeolite contact and affecting the pH of the solutionwill be considered below:

a- Hydrolysis of zeolite: this occurs at low pH since the zeolite structure may be adversely affected by acids (Ibrahim, 2001).

b- Hydrolysis of metal ions: this results in lowering the pH (increased acidity).

c- Release of exchangeable alkaline metal ions from active site at the zeolite surface: the addition of Na^+ and possibly some K^+, Ca^{2+} or Mg^{2+} to the solution will drive the pH up (more alkalinity). Sodium ions are dominant because they have been added to the mineral in the preparation step to activate its sites for ion exchange.

d- Uptake of metal ions by zeolite: removal of cationic Cr(III) species will raise the pH (reduce acidity).

e- Uptake of protons or hydronium ions: removal of H^+ (or H_3O^+) will decrease solution acidity.

f- Dissolution of solid carbonate and hydroxide impurities in the zeolite tuff: these impurities will also contribute to the rise of pH.

The net pH value, measured at a given time, is the resultant of the effects of two or more processes working in opposite direction. Since the final pH is always higher than the initial pH (of solid-free solution), it seems that processes (c), (d) and (f) are more influential thus pushing the pH scale up to the alkaline side.The sharp rise in pH during the initial sorption stage is understood noting that the release of Na^+ ions into solution is an easy process due to their accessibility on the external surface of zeolite. Moreover, the rates of mass transfer are always high in the first few minutes due to the higher driving force of concentration difference at the solid-liquid interface. At later stages, the driving forces decrease and the pH level is stabilized.

3.4. Cr(III) Uptake Mechanism

The mechanism of Cr(III) uptake by zeolite tuff can be explored in the light of the chemistry of Cr(III) aquo-species which is strongly dependent on pH. Like many metal ions, the chromium cation Cr^{3+}, which is obtained from the ionization of hydrous chromium chloride salt in water, undergoes hydrolysis by reactions with water molecules to give different hydrated ions at different pH levels. The following equations represent the hydrolysis reactions (Rai, *et al.*, 1987; Leyva-Ramos *et al.*, 2004); the pK value for each is provided below (K is the ionic equilibrium constant):

$Cr^{3+} + H_2O \leftrightarrow Cr(OH)^{2+} + H^+$ (7) $pK_1 = 3.83$ (7)

$Cr^{3+} + 2\,H_2O \leftrightarrow Cr(OH)_2^{\,+} + 2\,H^+$ (8) $pK_2 = 10.06$ (8)

$Cr^{3+} + 3H_2O \leftrightarrow Cr(OH)_3^{\,0} + 3H^+$ (9) $pK_3 = 18.70$ (9)

$Cr^{3+} + 4H_2O \leftrightarrow Cr_3(OH)_4^{\,5+} + 4\,H^+$ (10) $pK_4 = 8.40$ (10)

The mechanism of Cr(III) uptake by zeolite tuff can be explored in the light of the chemistry of Cr(III) aquo-species which is strongly dependent on pH. Like many metal ions, the chromium cation Cr^{3+}, which is obtained from the ionization of hydrous chromium chloride salt in water, undergoes hydrolysis by reactions with water molecules to give different hydrated ions at different pH levels. The following equations represent the hydrolysis reactions (Rai, 1987; Leyva-Ramos *et al.*, 1995); the pK value for each is provided below (K is the ionic equilibrium constant):

Fig. 11 is the speciation diagram of Cr(III) in dilute aqueous solutions(Leyva-Ramos *et al.*, 1995; Bradl, 2004). This is a plot of percent molar concentration of each aquo-species versus pH indicating which species is dominant at a given pH. Fig. 10 indicates that the pH range investigated in this work was from 4.0 to 7.0 and thus two regions in Fig. 11 are of particular interest:

i) Region of pH 4.0 to 6.0: The chromium species $Cr(OH)_2^{\,+}$produced by the first hydrolysis reaction represented by equation 8 is dominant (50% at pH 4.0 rising to 70% at pH 4.5-5.0 then decreasing to 40% at pH 6.0). The co-existing Cr^{3+}cation has strong tendency to form stable complexes with H_2O molecules and ligands (particularly Cl^-, the counter ion of Cr^{3+} in chromium chloride) such as $[Cr(H_2O)_6]^{3+}$ which may further undergo hydrolytic polymerization to give more complicated complex ions with larger size and charge (Richens, 1997). Therefore, it is suggested that $Cr(OH)^{2+}$ is the ion mainly removed in this pH range by ion exchange as can be represented by the following chemical equation:

$Cr(OH)^{2+}_{(aq)} + 2\,Na^+\,(Z) \rightarrow Cr(OH)^{2+}\,(Z) + 2\,Na^+_{(aq)}$ (11)

This does not, however, exclude the possibility of exchanging, to a lesser extent, other cationic species existing in this region for zeolite sodium ions.The average pore diameter of the investigated size cuts of zeolite is 1.75 Å (Table 1) indicating a microporous structure. According to Nightingale (1959) and Pauling (1970), the hydrated ionic radius of Cr(III) is estimated to be 9.0 Å which is five times as large. Therefore, it can be concluded that these ions are attached to the external surface of zeolite particle and would not be able to penetrate inside the porous structure. This stage of metal uptake is very fast since the final pH exceeds 6.0 in less than 10 minutes as shown in Fig. 11.

ii) Region of pH > 6.0: The published data in many sources supports the event of chemical precipitation of trivalent chromium as hydroxide at moderately acidic conditions. According to Leyva-Ramos *et al.* (2004), Cr(III) precipitates as $Cr(OH)_3$ at pH 6.4 from solutions having up to 20 mg/L. According to Lurie (1975), precipitation of $Cr(OH)_3$ starts at 4.9 from high concentration of Cr(III) of 0.01 M (equivalent to 520 mg/L). At the intermediate concentrations tested in this study's experiments (50-100 mg/L as C_o), chemical precipitation is likely to start around pH 6.0 which is an intermediate value of acidity.

The above discussion reveals that two main mechanisms of uptake are plausible: (a) ion exchange of cations species especially $Cr(OH)^{2+}$ in the initial stage before reaching pH 6.0; and (b) adsorption on external particle surface of fine $Cr(OH)_3$ particles formed by chemical precipitation at pH > 6.0. The total monolayer coverage deduced from Langmuir isotherm fitting would should include all Cr(III) species removed by both mechanisms.

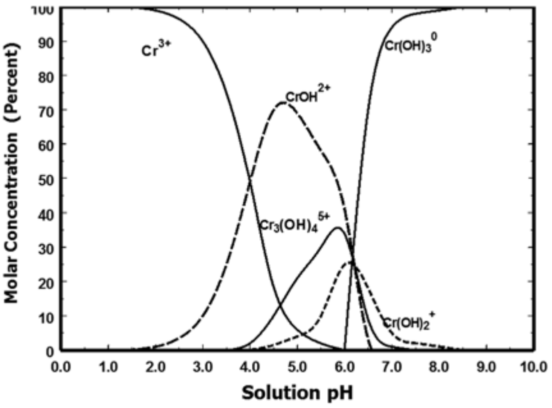

Figure 11: Speciation of chromium in aqueous solutions at 25°C

4. Conclusions

Based on data analysis and discussion of the experimental results of this study on Cr(III) removal by Jordanian NaCl-activated natural zeolite, it can be concluded that trivalent chromium is possibly removed from aqueous solutions up to 99% using phillipsite-rich zeolitetuff which appears to be a cost-effective adsorbent.The zeolite dose and initial Cr(III) ion concentration are key factors influencing equilibrium uptake.Equilibrium pH increased linearly with zeolite dose at a given initial Cr(III) concentration.Breakthrough curves demonstrated the applicability of the tested zeolite mineral in continuous fixed-bed column operation and breakpoint times up to 2.5 hours were obtained at 5% breakpoint.

Nomenclature

A_R: Redlich-Peterson parameter (mg/L)

B_R: Redlich-Peterson parameter (L/mg)

b: Langmuir isotherm parameter related to adsorption energy (L/mg)

C_o: Initial Cr ions concentration (mg/L)

C_e: Equilibrium Cr ions concentration (mg/L)

g: Exponent of Redlich-Peterson isotherm

H: Height of fixed-bed of zeolite, cm

K_F: Freundlich isotherm parameter related to adsorption capacity (L/mg)

n: Freundlich isotherm parameter related to adsorption intensity (dimensionless)

q_e: Equilibrium adsorption capacity (mg Cr(III)/g zeolite)

Q_L: Langmuir isotherm parameter related to adsorption capacity (mg/g)

R^2: Correlation coefficient obtained from linear regression

u: Solution velocity (flow rate divided by column cross-sectional area) (cm/min)

Z: Symbol representing active sites on the zeolite surface.

References

[1] Adriano, B.C., 2001. Trace Elements in Terrestrial Environments: Biogeochemistry, Bioavailability and Risks of Metals. Springer-Verlag, Berlin.

[2] Al-Haj-Ali, A. and Al-Hunaidi, T., 2004. Breakthrough Curves and Column Design Parameters for Sorption of Lead Ions by Natural Zeolite, Environmental Technology, 25:1009- 1019.

[3] Al-Haj-Ali, A. and El-Bishtawi, R., 1997. Removal of Lead and Nickel Ions Using ZeoliteTuff, Journal of Chemical Technology and Biotechnology, 69: 27- 34.

[4] Alvarez-Ayuso, E., Garcia-Sanchez, A. and Querol, X., 2003. Purification of Metal Electroplating Wastewaters Using Zeolites, Water Research, 37: 4855- 4862.

[5] Baker, H.M.,Massadeh, A.M. and Younes, H. A., 2009. Natural Jordanian Zeolite: Removal of Heavy Metal Ions from Water Samples Using Column and Batch Methods, Environmental Monitoring and Assessment, 157(1-4):319-30.

[6] Bradl, H. B., 2004. Adsorption of Heavy Metal Ions on Soils and Soils Constituents. Journal of Colloidal and Environmental Geology, 277:1-18.

[7] Ibrahim, K. and Jbara, H., 2009. Removal of paraquat from synthetic wastewater usingphillipsite–faujasite tuff from Jordan, Journal of Hazardous Materials, 163, 82-86.

[8] Ibrahim, K., 2001. Evaluation of Jordanian faujasite tuff by comparison with other natural and synthetic zeolite, Environmental Geology, 40 (4-5): 440-445

[9] Ibrahim, K., Nasser Ed-Deen, T. and Khoury, H., 2002. Use of Natural Chabazite- PhillipsiteTuff in Wastewater Treatment from Electroplating Factories in Jordan, Environ Geology, 41: 547- 551.

[10] Karatas, M., 2012. Removal of Pb(II) from Water by Natural ZeoliticTuff: Kinetics and Thermodynamics, Journal of Hazardous Materials, 199–200: 383–389.

[11] Kirk-Othmer. 2007. Kirk-Othmer Encyclopedia of Chemical Technology, 5th Ed, John Wiley, New York.

[12] Leyva-Ramos, R.; Fuentes-Rubio, L; Maria Guerrero-Coronado, R. and Mendoza-Barron, J., 2004. Adsorption of Trivalent Chromium from Aqueous Solutions onto Activated Carbon, Journal of Chemical Technology andBiotechnology, 62:64-67.

[13] Luri, J., 1975. Handbook of Analytical Chemistry. Mir Publishers, Moscow.

[14] Malamisa, S and Katsou, E., 2013. A Review on Zinc and Nickel Adsorption on Natural and Modified Zeolite, Bentonite and Vermiculite: Examination of Process Parameters, Kinetics and Isotherms, Journal of Hazardous Materials, 252–253: 428–461

[15] Natural Resources Authority of Jordan, 2006. Mineral Status and Future Opportunity: Zeolitic Tuff, prepared by Nawasreh, M. K.; Yasin, S.M. and Zurquiah, N.A., pp. 21, available athttp://www.nra.gov.jo,Accessed April, 9th, 2014.

[16] Nightingale, E. R., 1959. Phenomenological Theory of Ion Solvation: Effective Radii of Hydrated Ions, the Journal of Physical Chemistry, 63(9)1381- 1387.

[17] Obiri-Nyarko, F., Grajales-Mesa, F. G., Malina, G., 2014. An Overview of Permeable Reactive Barriers for In-situ Sustainable Groundwater Remediation, Chemosphere, 111: 243–259

[18] Pauling, P., 1970. General Chemistry. W H Freeman, New York.

[19] Rai, D., Sass, B. M. and Moore, D. A., 1987. Chromium (III) Hydrolysis Constants and Solubility of Chromium (III) Hydroxide, Inorganic Chemistry, 26: 345- 349.

[20] Redlich, O. and Peterson, D. L., 1959. A Useful Adsorption Isotherm, Journal of Physical Chemistry, 63: 1024-1024.

[21] Reynolds, T., Richards, P., 1996. Unit Operation and Process in Environmental Engineering, 3rd Ed., PWS, Boston, USA.

[22] Richens, D.T., 1997. The Chemistry of Aqua Ions. John Wiley, Chichester, UK.

[23] Stumm, W. and Morgan, J.J., 1996. Aquatic Chemistry: Chemical Equilibria and Rates in Natural Waters. 3rd Ed., John Wiley, New York.

[24] Taamneh, Y. and Al Dwairi, R., 2013.The Efficiency of Jordanian Natural Zeolite for Heavy Metals Removal, Applied Water Science, 3:77–84.

[25] Wang, S. and Peng, Y., 2010. Natural Zeolites as Effective Adsorbents in Water and Wastewater Treatment, Chemical Engineering Journal, 156 (1): 11-24.

[26] WHO, 2011. Guidelines for Drinking Water Quality.4thEd. World Health Organization, Geneva.